Laser action in ZnO nanoneedles selectively grown on silicon and plastic substrates

S. P. Lau,[a] H. Y. Yang, S. F. Yu, and H. D. Li
School of Electrical and Electronic Engineering, Nanyang Technological University, Nanyang Avenue, Singapore 639798

M. Tanemura, T. Okita, and H. Hatano
Department of Environmental Technology, Graduate School of Engineering, Nagoya Institute of Technology, Gokiso-cho, Showa-ku, Nagoya 466-8555, Japan

H. H. Hng
School of Materials Engineering, Nanyang Technological University, Nanyang Avenue, Singapore 639798

(Received 23 March 2005; accepted 24 May 2005; published online 28 June 2005)

An ion-beam technique has been employed to fabricate nanoscale needlelike structures in ZnO thin films on silicon and plastic substrates at room temperature. The ZnO nanoneedles showed a single-crystalline wurtzite structure, the stem of which was around 100 nm in diameter. The sharp tips of the nanoneedles exhibited an apex angle of 20° as measured by transmission electron microscopy. Room-temperature ultraviolet random lasing action was observed in the ZnO nanoneedle arrays under 355 nm optical excitation. © *2005 American Institute of Physics*.
[DOI: 10.1063/1.1984106]

One-dimensional (1D) semiconductor nanostructures are expected to provide functional components for future electronic, optoelectronic, and nanoelectromechanical systems.[1] There has been considerable interest in the growth of 1D semiconductor nanostructures on silicon substrates as well as temperature-sensitive substrates like plastic. The use of Si substrates enables the integration of nanomaterials in Si-based electronic devices. It is also desirable to fabricate semiconductor nanostructures on plastic substrates as it enables the development of high-performance electronic and photonic devices with the potential to impact a broad spectrum of applications.[2] Despite significant progress in deposition techniques such as vapor-liquid solid (VLS),[3] thermal evaporation condensation,[4] and metalorganic chemical-vapor deposition (MOCVD),[5] the synthesis of semiconductor nanostructures still requires growth temperatures of above 400 °C. Here, we report the growth of aligned ZnO nanoneedles on Si and plastic substrates using a simple ion-beam technique. In principle, this technique is capable of fabricating a desired type and size of nanostructure on any solid substrate.[6,7] As 1D ZnO nanostructures have attracted considerable attention due to their optical properties and potential application in nanoscale photonics,[8] it is of significant interest in fabricating ZnO nanostructures directly on plastic substrates. Although low-temperature (<100 °C) aqueous-solution-based synthesis methods have been demonstrated to grow aligned ZnO nanostructures, a seed layer is required which may lead to contamination.[9,10] The ion-beam technique should lead to a new approach to fabricate semiconductor nanostructures selectively on any substrate, especially on temperature-sensitive substrates, which may find applications in the emerging plastic electronic and optoelectronic devices.

ZnO epilayers were grown using the filtered cathodic vacuum arc (FCVA) technique. The apparatus of the FCVA has been described elsewhere.[11] High-purity zinc (99.9% purity) was used as the cathode material and oxygen gas was used as the reactant gas. Typically, the base pressure was kept at approximately 2.7×10^{-4} Pa, and the pressure during deposition was about 1.3×10^{-2} Pa. An arc current of 60 A was used to generate the plasma, and the axial and curvilinear fields were produced by a magnetic field of strength about 40 mT to steer the plasma. The ZnO thin films were deposited at a substrate temperature of 200 °C onto Si and plastic substrates.

The ZnO nanostructures were fabricated by an ion-beam system comprised of an ultrahigh vacuum scanning electron microscope (UHV-SEM) (JEOL; JAMP-10S) and a differentially pumped microbeam ion gun (JEOL; MIED). The sputtering was done with 3 keV Ar^+ ions focused into a microbeam 380 μm in diameter with mean ion-current densities of 220 $\mu A/cm^2$. A thin carbon film was deposited prior to sputtering to enhance the ion-induced formation of nanostrucures.[12] Ion irradiation was carried out at room temperature for 30 and 60 min. The residue of carbon layer was then removed by ethanol before characterization. Optical characteristics of the devices at room temperature were studied under optical excitation by a 355-nm frequency tripled Nd:YAG (yttrium aluminum garnet) pulse laser (10 Hz, 6 ns pulse width). Optical pump was achieved by using a cylindrical lens to focus a pump stripe of 5 mm length and 60 μm width onto the sample. A polarizer was set before the detector in order to analyze the polarization properties of the lasing light.

We shall first illustrate the fabrication of ZnO nanoneedles on silicon substrates. The key steps in the fabrication process include (i) the deposition of a 420-nm-thick SiO_2 on Si by thermal oxidation; (ii) the deposition of a 300-nm-thick ZnO film; (iii) the deposition of a thin carbon layer to enhance the ion-induced formation of nanostructures; and (iv) the irradiation of the sample by Ar^+ ion beam at room temperature. The ZnO nanostructures were formed selectively and uniformly on the ZnO surface. The growth mechanism

[a]Author to whom correspondence should be addressed; electronic mail: esplau@ntu.edu.sg

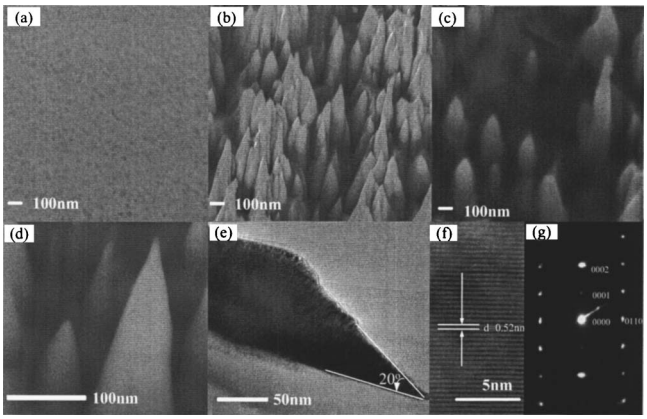

FIG. 1. (a) SEM image of the as-grown ZnO thin film. SEM images of the ZnO nanoneedle arrays after (b) 30 min and (c) 60 min ion irradiation. (d) High magnification SEM image of the ZnO nanoneedles. (e) TEM image of a single nanoneedle. (f) High-resolution TEM image of the nanoneedle and (g) the corresponding electron-diffraction pattern.

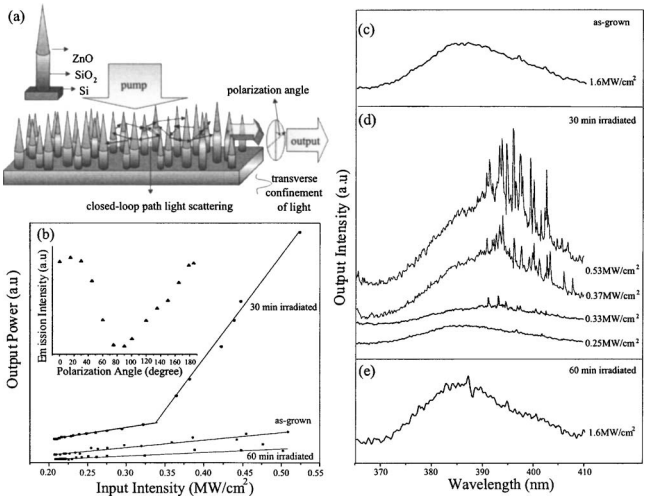

FIG. 2. (a) Schematic diagram of the laser measurement setup. (b) Light-light curves of the samples after various ion irradiation times. The inset shows the maximum emission intensity of the TE mode as a function of polarization angles. (c) Emission spectrum of the as-grown ZnO thin film under pump power of 1.6 M/cm^2. (d) Evolution of emission spectra of the 30-min irradiated sample under different pump intensities. (e) Emission spectrum of the sample irradiated for 60 min under pump power of 1.6 M/cm^2.

of ZnO nanoneedles may be similar to the sputter-induced CNFs, as reported by Tamenura *et al.*[12] The formation of nanoneedles is ascribed to the dependence of sputtering yield on the incidence angle of ion-beam measured from the normal to the surface. The thick SiO_2 layer ensures the confinement of the light in a waveguide structure for the laser action measurement.

Figure 1(a) shows the SEM image of the as-grown ZnO thin film. Figures 1(b) and 1(c) show the aligned ZnO nanoneedles formed after 30 and 60 min ion-beam irradiation, respectively. No features were observed from the as-grown ZnO thin film. After ion irradiation, sharp tips of conelike structures were clearly seen [Fig. 1(d)]. The lengths of the cone structures ranged from 200 to 400 nm. The diameter of the nanoneedles in the stem part was around 100 nm, where some of the nanoneedles tend to form in a cluster with similar sharpness at the tip. As the ZnO thin film was only 300 nm thick, the upper part of the cone was ZnO [white contrast as shown in Fig. 1(d)] and the lower part of the stem was SiO_2. It can be seen that the separation between the nanoneedles was irregular and ranged from a few nanometers to tens of nanometers. The density of the nanoneedles under 30 min irradiation was much higher than the sample irradiated for 60 min, as shown in Figs. 1(b) and 1(c). Energy-dispersive x-ray spectroscopy (EDX) was used to investigate the residue material between the nanoneedles, but no contaminant was detected. Figure 1(e) shows the TEM image of an individual nanoneedle. The tips of the nanoneedles exhibited an extremely sharp morphology. The interior angle of the nanoneedles was around 20°. The sharpness of the tip was comparable to the ZnO nanoneedles prepared by catalyst-free MOCVD (Ref. 5). Electron diffraction and high-resolution TEM observations indicated that the nanoneedles were in fact single crystals and were indexed to be the wurtzite structure of ZnO with lattice constants of $a=0.32$ nm, $c=0.52$ nm [Figs. 1(f) and 1(g)]. This result shows that the nanoneedles maintained the high-crystal quality of the ZnO thin film.

Room-temperature optical characteristics of ZnO nanoneedles were studied under an optical excitation. Figure 2(a) shows the experimental setup. Figure 2(b) shows the light-light curves of the samples. Only the sample irradiated for 30 min showed a "kink" in the light-light curves which was characteristic of laser action. As shown in Figs. 2(c) and 2(e), the as-grown and 60-min-irradiated samples showed only amplified spontaneous emission (ASE) spectra with a peak wavelength and full width at half maximum (FWHM) of about 385 and 12 nm, respectively, at a pump intensity of 1.6 MW/cm^2. Figure 2(d) shows the evolution of emission spectra of the ZnO nanoneedles sample irradiated for 30 min as a function of pump power. Below the threshold, ASE was observed. When the pump power reached a threshold as high as 0.34 MW/cm^2, a dramatic emission oscillation in a linewidth as narrow as 0.4 nm emerged from the single-broad emission spectra. As the pump power increased, multiple laser modes with strong coherent feedback at wavelengths between 390 and 400 nm were detected. This phenomenon of emission spectra was attributed to random lasing with coherent feedback.[13,14] Conventional lasing due to the Fabry-Perot (FP) cavities between the top and bottom natural facets of the ZnO nanoneedles was unlikely to occur. This is because the short length (<300 nm) and the sharp top surface of the ZnO nanoneedles were not able to provide sufficient optical gain and large optical loss, respectively. Hence, the natural FP cavities of the ZnO nanoneedles would not sustain lasing even under a high optical excitation. Random laser does not require a regular cavity but depends instead on a scattering material. Random laser action is possible for the ZnO nanoneedles as the corresponding gain length and scattering mean-free path along the lateral direction satisfy the requirements of random laser action; that is, the gain length (scattering mean-free path) is long (short) enough to sustain amplified coherent feedback.[14] Due to the fact that the ZnO nanoneedles were grown on a SiO_2/Si substrate, the refractive index difference in the interface of air $(n_r=1)/ZnO(n_r \sim 2.1)/SiO_2(n_r \sim 1.45)$ allowed strong scattering and amplification along the ZnO tips to achieve random laser action. Above the threshold, the emission was strongly polarized, as shown in the inset of Fig. 2(b). Random laser action has been observed in ZnO thin films annealed at 900 °C and ZnO nanorod arrays embedded in ZnO epilayers.[15,16] The thresh-

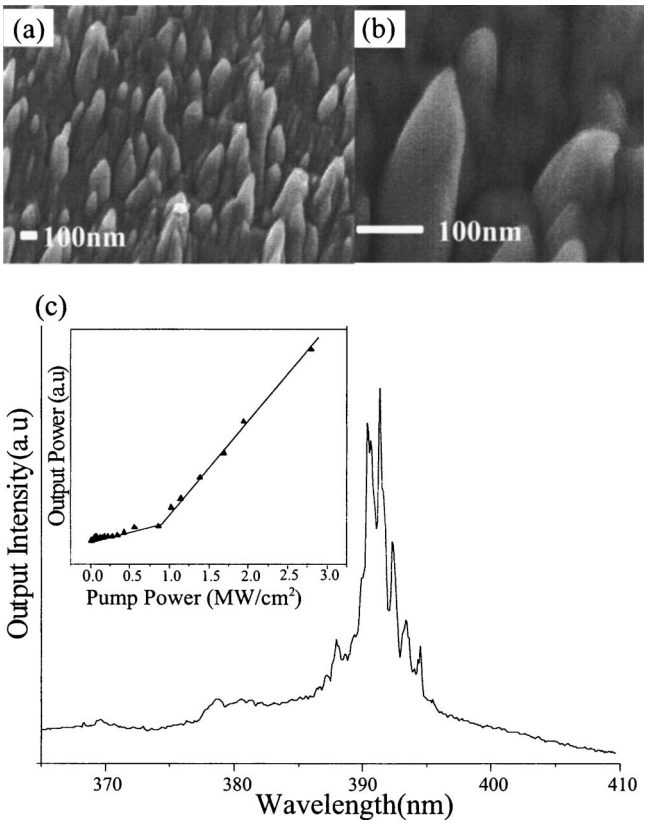

FIG. 3. (a) Low and (b) high magnification SEM images of ZnO nano needles on plastic substrate. (c) Emission spectrum under 2.8 MW/cm^2 pump intensity. The inset shows the light-light curve of ZnO nanoneedles on plastic substrate.

old pump intensity of the ZnO nanoneedles (0.35 MW/cm^2) was comparable to that of ZnO thin films annealed at 900 °C (0.32 MW/cm^2), but it was significantly lower than that of ZnO nanorod arrays embedded in ZnO epilayers (0.8 MW/cm^2). The relatively lower pump threshold of the ZnO nanoneedles compared to that of ZnO nanorod arrays was due to the relatively stronger optical scattering between the air and ZnO interface of the ZnO nanoneedles [Fig. 1(b)], so that coherent optical feedback could be obtained from relatively low pump intensities. It should also be noted that the threshold pump intensity of ZnO nanoneedles random lasers was significantly lower than the conventional lasing observed in ZnO nanocolumns prepared by an aqueous solution method (3 MW/cm^2) (Ref. 9). Our result was also significant as no high-temperature annealing was required in order to form random media in the ZnO thin films. The sample under 60 min irradiation exhibited no lasing. This was attributed to the low density of nanoneedles, which did not satisfy the requirement of random laser action.

A similar approach was used to fabricate ZnO nanoneedles on flexible plastic substrates. We used 180-μm-thick commercially available Kapton® polyimide foil as the flexible substrate material. Polyimide foils are commonly used as substrate material for flexible thin-film transistors.[17] A 520-nm-thick ZnO was deposited on the plastic substrate at 200 °C. Figures 3(a) and 3(b) show the SEM images of the ZnO nanoneedles on the plastic substrate. The cone-shape morphology was also obtained after 30 min of ion irradiation. The lengths and diameter (stem) of the nanoneedles were 200–300 nm and 100 nm, respectively, which were very similar to the ZnO nanoneedles on Si substrate [Fig. 3(b)]. However, the tips of the nanoneedles were not as sharp as those for the Si sample, which might be due to the quality of the ZnO film and the softness of the plastic substrate.

The optical characterization of the plastic sample was studied. Figure 3(c) shows the emission spectrum of the nanoneedles on the plastic substrate excited above the threshold at 2.8 MW/cm^2. Random laser action with coherent feedback was clearly detected and the resulting threshold pump power density was determined to be 0.84 MW/cm^2 as shown in the inset of Fig. 3(c). The lasing threshold of the plastic sample was two times more than that of the nano needles on Si (i.e., 0.34 MW/cm^2). As illustrated in Fig. 3(a), the ZnO nanoneedles were about 300 nm in length, and there was a 200-nm-thick ZnO thin film underneath the nanoneedles so that light could be confined within the ZnO nanoneedle array. However, the relatively high pump intensity of the plastic sample was mainly due to the high optical loss of the substrate as the polyimide substrate absorbed the light with wavelength less than 450 nm. As a result, the corresponding pump threshold was higher than that with Si substrate. Despite all these, random laser action in the ZnO nanoneedles could still be obtained, which demonstrated the usefulness of the ion-beam technique for creating functional nanostructures on flexible plastic substrates.

In summary, we have demonstrated the fabrication of ZnO nanostructures directly on Si and plastic substrates using the ion-beam technique. Random laser action could be observed from samples on both Si and plastic substrates.

This work was partly supported by the Agency for Science, Technology and Research of Singapore (Project No. 022-101-0033), the Japan Society for the Promotion of Science (JSPS; Grants-in-Aid for Scientific Research B, No. 15360007), and the NITECH 21st Century COE Program "World Ceramics Center for Environmental Harmony."

[1] C. M. Lieber, MRS Bull. **28**, 486 (2003).
[2] M. C. McAlpine, R. S. Friedman, S. Jin, K. H. Lin, W. U. Wang, and C. M. Lieber, Nano Lett. **3**, 1531 (2003).
[3] M. H. Huang, Y. Wu, H. Feick, N. Tran, E. Weber, and P. Yang, Adv. Mater. (Weinheim, Ger.) **13**, 113 (2001).
[4] B. D. Yao, Y. F. Chan, and N. Wang, Adv. Mater. (Weinheim, Ger.) **81**, 757 (2002).
[5] W. Park, C. Yi, M. Kim, and S. Pennycook, Adv. Mater. (Weinheim, Ger.) **14**, 1841 (2002).
[6] M. Tanemura, H. Yamauchi, Y. Yamane, T. Okita, and S. Tanemura, Nucl. Instrum. Methods Phys. Res. B **215**, 137 (2004).
[7] M. Tanemura, T. Okita, H. Yamauchi, S. Tanemura, and R. Morishima, Appl. Phys. Lett. **84**, 3831 (2004).
[8] M. H. Huang, S. Mao, H. Feich, H. Yan, Y. Wu, H. Kind, E. Weber, R. Russo, and P. Yang, Science **292**, 1897 (2001).
[9] K. Govender, D. S. Boyle, P. O'Brien, D. Binks, D. West, and D. Coleman, Adv. Mater. (Weinheim, Ger.) **14**, 1221 (2002).
[10] J. B. Cui, C. P. Daghlian, U. J. Gibson, R. Pusche, P. Geithener, and L. Ley, J. Appl. Phys. **97**, 044315 (2005).
[11] Y. G. Wang, S. P. Lau, H. W. Lee, S. F. Yu, B. K. Tay, X. H. Zhang, K. Y. Tse, and H. H. Hng, J. Appl. Phys. **94**, 1597 (2003).
[12] M. Tanemura, J. Tanaka, K. Itoh, Y. Fujimoto, Y. Agawa, L. Miao, and S. Tanemura, Appl. Phys. Lett. **86**, 113107 (2005).
[13] H. Cao, Y. G. Zhao, H. C. Ong, S. T. Ho, J. Y. Dai, J. Y. Wu, and R. P. H. Chang, Appl. Phys. Lett. **73**, 3656 (1998).
[14] H. Cao, Waves Random Media **12**, R1 (2003).
[15] S. F. Yu, C. Yuen, S. P. Lau, and H. W. Lee, Appl. Phys. Lett. **84**, 3244 (2004).
[16] S. F. Yu, C. Yuen, S. P. Lau, W. I. Park, and G. C. Yi, Appl. Phys. Lett. **84**, 3241 (2004).
[17] H. Gleskova, S. Wagner, and Z. Suo, Appl. Phys. Lett. **75**, 3011 (1999).